Determination of photon efficiencies and hydrocarbon influxes in the detached outer divertor plasma of ASDEX Upgrade

S. Brezinsek[1], R. Pugno[2], U. Fantz[2], A. Manhard[2], H.W. Müller[2], A. Kallenbach[2], Ph. Mertens[1], and the ASDEX Upgrade team

[1] *Institut für Plasmaphysik, Forschungszentrum Jülich, Association EURATOM-FZJ, Trilateral Euregio Cluster, Germany*

[2] *Max-Planck-Institut fr Plasmaphysik, Euratom Association, 85748 Garching bei München, Germany*

Abstract

Hydrocarbon injection experiments with in-situ calibration of spectroscopic signals have been carried out to determine the hydrocarbon flux and the chemical erosion yield under detached plasma conditions in ASDEX Upgrade. A plasma scenario was developed to detach the outer divertor in L-mode and to provide the recombining deuterium target plasma. A significant decrease of carbon-related intrinsic photon fluxes, in particular of the CH Gerö and of the C_2 Swan band was observed in detachment. Moderate methane/ethene injections were performed through a single gas valve and an increase of carbon-related intrinsic photon fluxes was detected which can be attributed to the amount of injected molecules. The experimentally determined effective inverse photon efficiencies are slightly larger than the ones deduced in attached plasmas. Nevertheless, the low intrinsic CH and C_2 light observed under detached conditions can still be attributed to a reduction of the hydrocarbon flux. The impact of detachment on the chemical erosion is discussed.

PACS: 52.70.Kz, 52.40.Hf, 52.25.Vy, 52.55.Fa, 33.20.Lg

1. Introduction

Carbon-fibre composite CFC is presently foreseen as plasma-facing material for the ITER divertor target plates [1]. CFC is chosen to sustain the high particle and heat flux loading during a reasonable number of transient events [2]. Apart from transient events, a reduction of the particle and heat flux in normal operation is forced to ensure a long lifetime of the plasma-facing components. A fully detached inner divertor and semi-detached outer divertor plasma [3] is the proposed ITER scenario to fulfil this requirement. However, the use of CFC is connected with erosion, transport and deposition of carbon [4] which leads with respect to safety to the critical issue of tritium co-deposition [5]. Reduction of the erosion process is desirable to ensure a large number of ITER discharges without cleaning intervention [6]. The influence of divertor detachment on the hydrocarbon chemistry is subject of present day research [7,8].

Experiments have been carried out to investigate the behaviour of the hydrocarbon particle flux and the chemical erosion yield in the outer divertor of ASDEX Upgrade under detached plasma conditions. The usually attached outer divertor leg which was recently identified to be the remaining source of carbon in ASDEX Upgrade [9] was detached on purpose. Injections of methane/ethene through a single gas valve were performed to determine effective inverse photon efficiencies or D/XB values [10-13] for different spectroscopic transitions, in particular the usually observed CH Gerö band and C_2 Swan band and, thus, to calibrate in-situ the photon fluxes of the corresponding break-up products. The low intrinsic hydrocarbon fluxes were quantified and a comparison of hydrocarbon photon and particle fluxes deduced in attached and detached divertor plasmas is presented. The effect of detachment on the chemical erosion is discussed.

2. Experimental set-up

A plasma scenario in lower single-null configuration and medium triangularity was devel-

oped to detach the outer divertor leg in high density L-mode discharges ($I_p = 0.8MA,\ B_t = 2.4T,\ n_e^0 = 6.0 \cdot 10^{19} m^{-3},\ T_e^0 = 1.5KeV,\ 1.2MW$ ICRH) with the aid of strong deuterium fuelling. The fuelling rate that was needed to establish a fully detached divertor, was determined in set-up discharges with density ramps. The transition from an attached to a detached divertor was observed by optical emission spectroscopy, and detected by the reduction of the ion flux Γ_{D^+} which was measured with the aid of a set of Langmuir Probes (LP) [14] located in the vertical target plates. The detached scenario was density-feedback controlled, providing a long flat-top phase of more than $4s$. Several discharges with high reproducibility were performed to vary the spectrometer settings and the injected species. Additionally, the back transition from the detached to the attached regime was investigated in discharges where the deuterium fuelling was stopped on purpose. Characteristic time traces are depicted in fig.1.

2.1 Local plasma conditions and settings in the outer divertor

Minor-perturbing methane/ethene injections of the order of $4.0 \cdot 10^{18} mol./s$ were made through the gas valve T3 (tube diameter: $0.4cm$) implemented in the vertical target plates ($T_{target} \simeq 350K$) of the outer divertor (fig.2). The injection of hydrocarbons allows to distinguish hydrogen (hydrocarbon catabolism) from deuterium (background plasma). The injected hydrocarbon did not lead to an increase of the hydrogen concentration in the plasma centre; the $H/(H+D)$ ratio lay between 3.0% to 4.0% for all discharges with strong fuelling. Plasma parameters at the injection location were varied by sweeping the position of the outer-strike point (OSP) about $10cm$. The injection was either into the private-flux region (PFR), the near or the far scrape-off layer (SOL). The long flat-top phase was sufficient to perform two sweeps in one discharge. One sweep was made with and one sweep without hydrocarbon injection. The later was used as reference to determine the intrinsic background under identical plasma conditions. Note that symmetric sweeping of the ISP and OSP is

comparable to vertical shift of the plasma column.

Local plasma parameters were measured with the aid of Langmuir probes and with Balmer spectroscopy observing the emission volume in front of the target plates (fig.2): Fig.3a shows the time evolution of the electron temperature T_e, the electron density n_e and Γ_{D^+} measured with LP and mapped to T3. The time points when the separatrix was on T3 are marked. The maximum in n_e is observed in the SOL away from the separatrix, this indicates an upward shift of the ionisation front which is characteristic for detached plasma conditions. T_e is almost constant at about $2eV$ during the sweep close to the LP detection limit. Analysis and simulation of Balmer recombination lines of the background species (fig.3b) provided $T_e \simeq 1.2eV$ and $n_e \simeq 3.0 \cdot 10^{20} m^{-3}$ in the volume. The outer divertor plasma was identified to be fully recombining.

2.2 Spectroscopic set-up

Atomic and molecular spectroscopy on hydrocarbon fragments was done with a set of fibre-coupled spectrometer systems, in particular with HAR and Echelle, which are briefly described here and in more detail elsewhere [15,16]. The HAR spectrometer ($1.0m$ Czerny-Turner spectrometer, grating: $1200l/mm$, spectral resolution: $R > 2.5 \cdot 10^4$, wavelength coverage: $\sim 8nm$, time resolution: $250ms$) was used for the time-resolved recording of the band heads of the CH Gerö band ($A - X$ transition) and the C_2 Swan band ($d - a$ transition) as well as for the CII multiplets at $426.7nm$ and at $515.0nm$. The Echelle spectrometer (cross-dispersion spectrometer, grating: $76l/mm$, spectral resolution: $R > 2 \cdot 10^4$, observed wavelength range: $345nm - 645nm$, exposure time: $250ms$) was chosen to record the complete molecular spectra of the Gerö and Swan band; the corresponding photon fluxes were deduced from fitted and simulated spectra [17]. Moreover, the hydrogen Balmer lines with $n \geq 4$ were measured simultaneously. However, the overview spectrum was recorded only for discrete time points.

All systems were equipped with one of three optical fibres (quartz, diameter: $0.1cm$) observing the same volume in front of the gas valve as shown in fig.2. This volume (VOL, elliptical cross-section: $5.6cm$ and $4.0cm$ diameter) was chosen large enough to ensure that a major part of emitted light from the different observed transitions was recorded. The cloud size was estimated by means of HAR, and four fibres from a set of discrete fibres (ROV, $1cm$ diameter) which were spatially separated over the divertor target plates. A correction factor of 1.5 to the photon fluxes deduced with VOL was applied in the case of injection into the detached plasma to take the loss of photons into account.

3. Experimental results

3.1 Spectroscopic observation and discussion

The detached divertor plasma leads in the first place to a reduction of the intrinsic photon flux of different carbon related transitions –in particular of CD, C_2 and CII– with respect to the attached divertor. Fig.4a/b illustrates the reduction of the CD Gerö band emission at the separatrix: the intrinsic photon flux $\phi_{A-X}^{CD\ int.}$ in detachment is diminished by more than a factor of 10 with respect to the attached reference (#20786). Note that, the BD $A-X$ band becomes very prominent in detachment and the P-branch interferes strongly with the CD Gerö band - in particular at the band head ($429.5-431.0nm$) where nearly half the emission is resulting from BD. This disturbance was considered in the spectral analysis.

Injection of CH_4 or C_2H_4 in the detached plasma leads to the appearance of the CH Gerö band (fig.4c). The inverse photon efficiencies for CH from CH_4 and C_2H_4 related to the complete electronic transition were determined for the injection close to the separatrix to $[D/XB]_{A-X}^{CH_4\rightarrow CH} = 18 \pm 7$ and $[D/XB]_{A-X}^{C_2H_4\rightarrow CH} = 47 \pm 19$, respectively. These D/XB values were deduced from the difference of the extrinsic and intrinsic photon flux as indicated in fig.4e for the C_2H_4 injection. Fig.4e shows the temporal evolution of band head intensity during the two OSP sweeps. However, hydrocarbon injection in attached plasmas leads to

a much stronger light emission of the CH Gerö band as depicted in fig.4d where C_2H_4 was injected in the attached phase of discharge #20785 ($T_e = 14eV$ and $n_e = 1 \cdot 10^{19} m^{-3}$ at the valve location). $[D/XB]_{A-X}^{C_2H_4 \rightarrow CH}$ amounts 19 ± 4 which is about 2.5 times lower than for detached plasma conditions. The photon efficiency for CH from CH_4 in L-mode discharges with divertor attachment ($n_e = 2...8 \cdot 10^{19} m^{-3}$, $T_e = 5...15eV$) was determined to $[D/XB]_{A-X}^{CH_4 \rightarrow CH} = 4 \ldots 15$ [19].

The C_2 Swan band shows a similar behaviour: the intrinsic photon flux $\phi_{d-a}^{C_2\ int.}$ is strongly suppressed in detached plasma conditions (fig.4f/g) and below the detection limit of the applied spectrometer system. Injection of C_2H_4 provides an increase of the C_2 Swan band emission. However, the effective inverse photon efficiencies $[D/XB]_{d-a}^{C_2H_4 \rightarrow C_2}$ differ significantly about 25 times: 16 ± 5 for the attached and 407 ± 134 for the detached case.

3.2 Hydrocarbon particle flux

The hydrocarbon influx $\Gamma_{C_xD_y}$ is given by the photon flux of the hydrocarbon representatives CD and C_2 and the corresponding D/XB-values. Two contributions to $\Gamma_{C_xD_y}$ have to be usually considered: one related to CD_y and one to C_2D_y [13]. Here, $\phi_{d-a}^{C_2\ int.}$ is below the detection limit of the Echelle spectrometer system in detached plasma conditions and we assume that the C_2D_y contribution can be neglected with respect to the CD_y contribution although the inverse photon efficiency is larger than in attached conditions. $\Gamma_{C_xD_y}$ can be described solely by CD_y, and thus, by the CD Gerö band.

In the following we focus on the hydrocarbon flux resulting from chemical erosion at the target plate close to the separatrix and $3.5cm$ deep in the SOL, and thus, close to the ionisation front. $\phi_{A-X}^{CD\ int.}$ increases in this spatial region from $4.5 \cdot 10^{18} \frac{ph}{m^2 s^1}$ -close to the separatrix- to $5.1 \cdot 10^{18} \frac{ph}{m^2 s^1}$ - in the SOL. Accordingly, the corresponding particle flux increases from 8.1 to $9.2 \cdot 10^{19} \frac{particles}{m^2 s^1}$, assuming that there is no isotope effect in the photon efficiencies for the CH and CD Gerö band.

In the case of the reference attached plasma both contributions to the hydrocarbon flux have to be taken into account. Consideration of only $\phi_{A-X}^{CD\ int.}$ and $[D/XB]_{A-X}^{CH_4 \rightarrow CH} = 10$ would lead to $6.0 \cdot 10^{20} \frac{particles}{m^2 s^1}$, whereas the total hydrocarbon flux including the contribution of C_2Dy is for typical L-mode conditions about a factor 1.3 larger, and amounts $7.8 \cdot 10^{20} \frac{particles}{m^2 s^1}$ [17].

We conclude that the strong photon flux reduction observed for these molecular transitions in the detached plasma suggest a strong reduction of the hydrocarbon particle flux coming from chemical erosion at the target. But the photon flux reduction is partially compensated by the increase of the corresponding inverse photon efficiency with respect to the attached plasma. Nevertheless a net-reduction of the hydrocarbon influx of about a factor 8 from attached to detached occurs.

4. Discussion and conclusion about Y_{chem}

The chemical erosion yield Y_C^{chem} is defined by the ratio of the hydrocarbon influx, thus particles eroded at the CFC target, to the outflux of mainly fuel particles which hit (perpendicularly) the CFC target plate. The influx is reduced in detached plasmas in comparison to attached plasmas, as presented in the previous section. The questions which have to be addressed are: (i) how is the fuel outflux defined in detached plasmas and (ii) which impact has the hydrocarbon flux reduction on Y_C^{chem}.

(i) The outflux has two contributions: the ion contribution Γ_{D^+} and the neutral particle contribution Γ_D. Ions and neutrals can chemically erode CFC under the assumption that no energetic threshold for the erosion process exist. Γ_{D^+} is the dominating part in the case of a full ionising plasma ($T_e > 5eV$) such as present in the attached outer divertor. In divertor detachment, neutrals can penetrate through the thin an cold separatrix and hit the CFC target. A large fraction of neutrals is present in the divertor and Γ_D is the dominating contribution. Typical values at the separatrix for L-mode discharges (#20784) are

$\Gamma_{D^+} \simeq 2 \cdot 10^{21} m^{-2} s^{-1} < \Gamma_D \simeq 2 \cdot 10^{22} m^{-2} s^{-1}$.

For a further analysis (of #20781-84) we concentrate on the local erosion yield in the region close to the separatrix and $3.5cm$ in the SOL. The deuterium outflux varies between $2.75 - 3.10 \cdot 10^{22} m^{-2} s^{-1}$ while the major fraction of this incident flux is determined by neutrals ($2.5 \cdot 10^{22} m^{-2} s^{-1}$). Here, we assume that the neutral flux to the target is about 50% of the neutral flux measured by ionisation gauges below the septum. This assumption is reasonable nearby the thin separatrix and up to the ionisation front where neutral particles cannot penetrate further in.

(ii) The measured hydrocarbon flux (sec.3) has to be related to the outflux discussed above to deduce the erosion yield at the CFC target. Y_{chem} varies between $2.9 - 3.0 \cdot 10^{-3}$ where the slightly higher yield is measured in the SOL. These values are comparable with predictions made with the outflux-dependent Roth formula [20]: $Y_{chem}^{Roth} = 2.5 - 3.2 \cdot 10^{-3}$. These calculations were done with the total outflux and under the assumption of a constant plasma background. A detailed modelling with an erosion-deposition code with an appropriate plasma background is in preparation but out of the scope of this paper. Note that the consideration of only Γ_{D^+} would lead to an erosion yield of $1.5 - 3.2 \cdot 10^{-2}$ with its maximum at the separatrix.

Acknowledgments

This work was done in the frame of the European Task Force on Plasma-Wall Interaction.

References

[1] Federici, G. et al., 2001 *Nucl. Fusion* **41** No. 12R

[2] Loarte, A. et al., 2006 this conference

[3] Kukushkin, A. et al., 2006 *J. Nucl. Mater.* at press

[4] V. Philipps et al., 2003 *Plasma Phys. Control. Fusion* **45** A17

[5] Counsell, G. et al., 2006 *Plasma Phys. Control. Fusion* at press

[6] Kirschner, A. et al., 2006 *J. Nucl. Mater.* at press

[7] Whyte, D. et al., 2001 *Nucl. Fusion* **41**1243

[8] Brezinsek, S. et al., 2006 *J. Nucl. Mater.* at press

[9] Kallenbach, A. et al., 2006 *J. Nucl. Mater.* at press

[10] Pospieszczyk, A. et al., 1989 *UCLA Report* PPG-1251

[11] Behringer, K. et al., 1990 *J. Nucl. Mater.* **176-177** 606

[12] Fantz, U. et al., 2001 *J. Nucl. Mater.* **290-293** 367

[13] Brezinsek, S. et al., 2004 *Physica Scripta* **T111** 42

[14] Weinlich, M., Carlson, A., 1997 *Phys. Plasmas* **4** 2151

[15] Pugno, R. et al., 2005 *J. Nucl. Mater.* **337-339** 985

[16] Manhard, A. et al., 2006 *Verhandlungen DPG*

[17] Fantz, U. et al., 2005 *J. Nucl. Mater.* **337-339** 1087

[18] Wünderlich, D., 2006 private communication

[19] Pugno, R. et al., 2003 *30th EPS Contr. Fus. and Plasma Phys., St. Petersburg* ECA Vol. 27A, P-1.153

[20] Roth, J. et al., 2004 *Nucl. Fusion* **44** L21

Figure captions:

Fig.1: Time traces of plasmas current, outer-strike point position, additional power, radiated power, central electron density, and neutral density in the divertor for the detached case (a) and the detached/attached case (b).

Fig.2: Schematic set-up: The range of the strike-point sweeping with respect to the injection valve T3 is indicated. The location of the Langmuir probes, the lines-of-sight of the spectroscopic systems, and the pressure gauges are presented.

Fig.3: a) Time resolved local plasma parameters at the target plates in the detached outer divertor recorded with Langmuir probes. b) Balmer-line spectrum of the fully recombining plasma. The plasma parameters in the volume in front of the target were deduced from Balmer-line ratio modelling [Wnderlich].

Fig.4: Comparison of the CH $A - X$ (a) and the C_2 $d - a$ spectrum (c) with and without local ethene injection under detached and attached plasma conditions, respectively. Time evolution of the CH Gerö (b) and C_2 Swan band head intensity (d) during the OSP sweep.

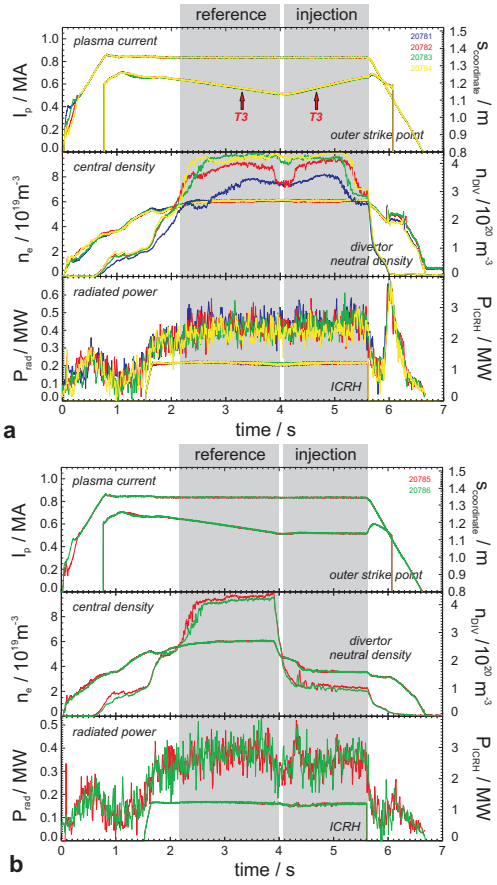
reference
injection
plasma current
20781
20782
20783
20784
T3
T3
outer strike point
central density
divertor
neutral density
radiated power
ICRH
time / s
a
reference
injection
plasma current
20785
20786
outer strike point
central density
divertor
neutral density
radiated power
ICRH
time / s
b

Figure 1:

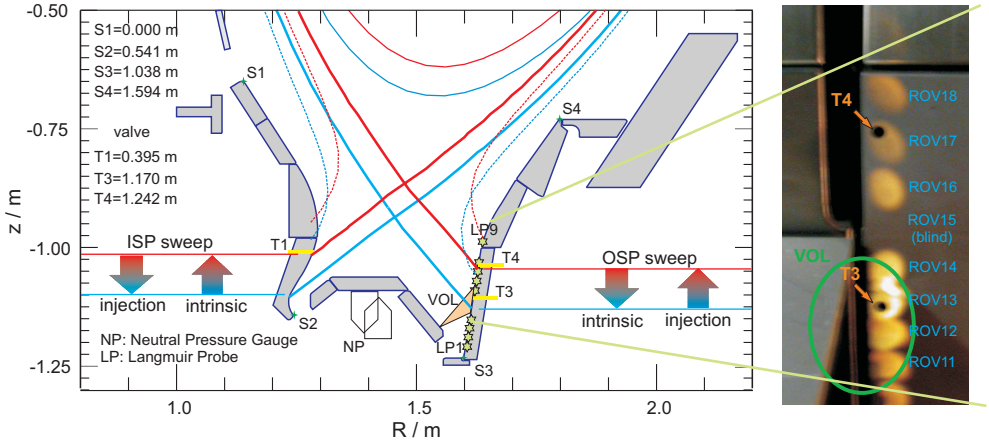
S1=0.000 m
S2=0.541 m
S3=1.038 m
S4=1.594 m
valve
T1=0.395 m
T3=1.170 m
T4=1.242 m
ISP sweep
injection
intrinsic
OSP sweep
intrinsic
injection
NP: Neutral Pressure Gauge
LP: Langmuir Probe
S1
S2
S3
S4
T1
T3
T4
VOL
NP
LP1
LP9
-0.50
-0.75
-1.00
-1.25
z / m
1.0
1.5
2.0
R / m
T4
ROV18
ROV17
ROV16
ROV15
(blind)
VOL
T3
ROV14
ROV13
ROV12
ROV11

Figure 2:

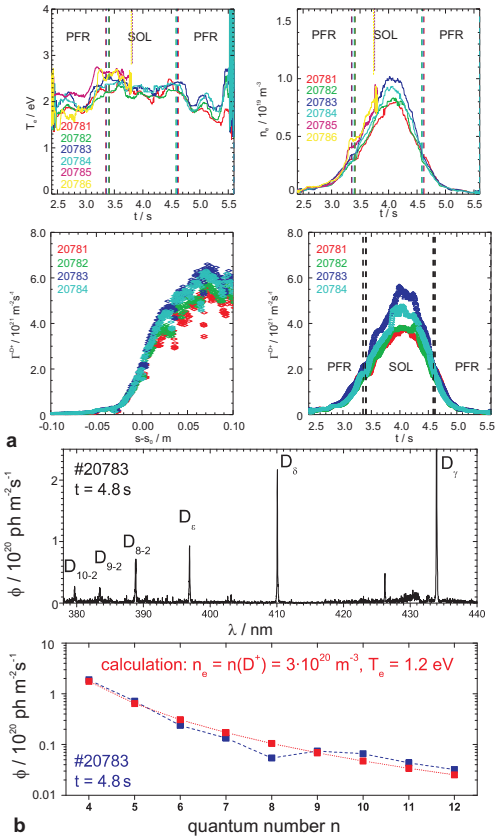
PFR
SOL
PFR
20781
20782
20783
20784
20785
20786
t / s
a
#20783
t = 4.8 s
D10-2
D9-2
D8-2
Dε
Dδ
Dγ
λ / nm
calculation: ne = n(D+) = 3·10^20 m^-3, Te = 1.2 eV
#20783
t = 4.8 s
quantum number n
b

Figure 3:

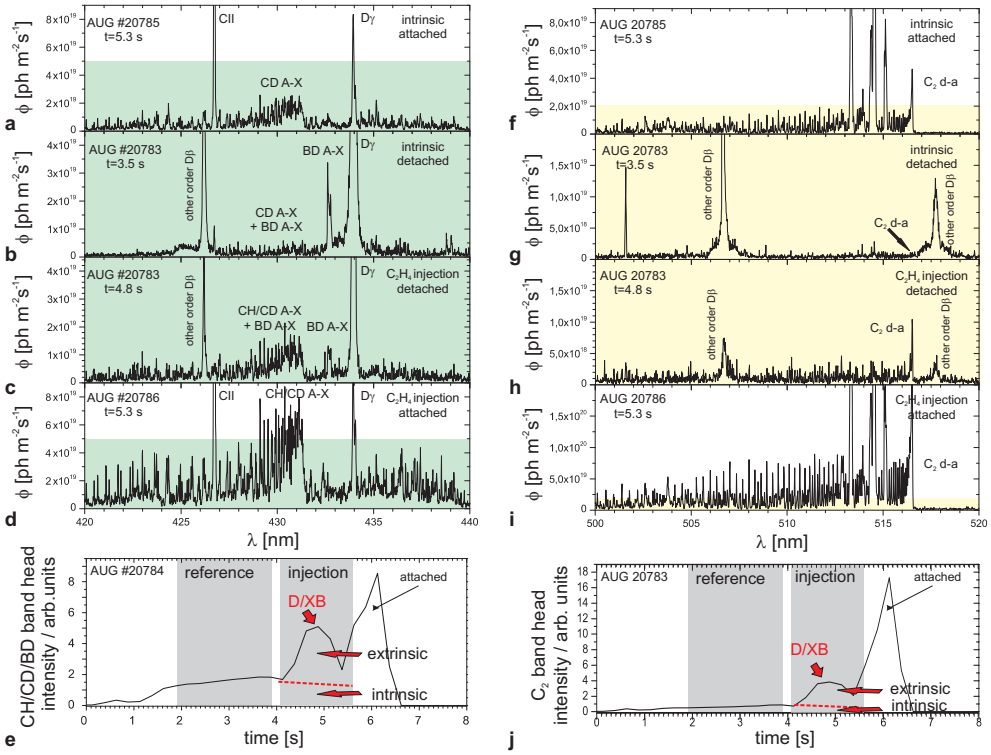
a
AUG #20785
t=5.3 s
CII
Dγ
intrinsic
attached
CD A-X
b
AUG #20783
t=3.5 s
other order Dβ
BD A-X
Dγ
intrinsic
detached
CD A-X
+ BD A-X
c
AUG #20783
t=4.8 s
other order Dβ
Dγ
C2H4 injection
detached
CH/CD A-X
+ BD A-X
BD A-X
d
AUG #20786
t=5.3 s
CII
CH/CD A-X
Dγ
C2H4 injection
attached
ϕ [ph m-2s-1]
λ [nm]
f
AUG 20785
t=5.3 s
intrinsic
attached
C2 d-a
g
AUG 20783
t=3.5 s
other order Dβ
intrinsic
detached
C2 d-a
other order Dβ
h
AUG 20783
t=4.8 s
other order Dβ
C2H4 injection
detached
C2 d-a
other order Dβ
i
AUG 20786
t=5.3 s
C2H4 injection
attached
C2 d-a
e
AUG #20784
reference
injection
attached
D/XB
extrinsic
intrinsic
CH/CD/BD band head
intensity / arb.units
time [s]
j
AUG 20783
reference
injection
attached
D/XB
extrinsic
intrinsic
C2 band head
intensity / arb. units
time [s]

Figure 4: